Chaos, Solitons and Fractals 41 (2009) 2553–2565

Contents lists available at ScienceDirect

Chaos, Solitons and Fractals

journal homepage: www.elsevier.com/locate/chaos

An analysis of heart rhythm dynamics using a three-coupled oscillator model

Sandra R.F.S.M. Gois, Marcelo A. Savi *

Universidade Federal do Rio de Janeiro, COPPE-Department of Mechanical Engineering, P.O. Box 68503, 21941972 Rio de Janeiro, RJ, Brazil

ARTICLE INFO

Article history:
Accepted 22 September 2008

ABSTRACT

Rhythmic phenomena represent one of the most striking manifestations of the dynamic behavior in biological systems. Understanding the mechanisms responsible for biological rhythms is crucial for the comprehension of the dynamics of life. Natural rhythms could be either regular or irregular over time and space. Each kind of dynamical behavior may be related to both normal and pathological physiological functioning. The cardiac conducting system can be treated as a network of self-excitatory elements and, since these elements exhibit oscillatory behavior, they can be modeled as nonlinear oscillators. This paper proposes a mathematical model to describe heart rhythms considering three modified Van der Pol oscillators connected with time delay couplings. Therefore, the heart dynamics is represented by a system of differential difference equations. Numerical simulations are carried out presenting qualitative agreement with the general heart rhythm behavior. Normal and pathological rhythms represented by the ECG signals are reproduced. Pathological rhythms are generated by either the coupling alterations that represents communications aspects in the heart electric system or forcing excitation representing external pacemaker excitation.

1. Introduction

Natural rhythms could be either regular or irregular over time and space. Each kind of dynamical behavior related to biomedical systems may be associated with both normal and pathological physiological functioning. Extremely regular dynamics may represent diseases including periodic breathing, certain abnormally heart rhythms, cyclical blood diseases, epilepsy, neurological tics and tremors. On the other hand, there are phenomena where regular dynamics reflect healthy behavior as sleep–wake cycle and menstrual rhythms. Moreover, irregular rhythms can also reflect disease: cardiac arrhythmias, such as fibrillation, and different neurological disorders are some examples [8,11,24,25,29].

Rhythmic changes of blood pressure, heart rate and other cardiovascular measures indicate the importance of dynamical aspects in the comprehension of cardiovascular rhythms. Several studies are pointing to the fact that certain cardiac arrhythmias are instances of chaos [22,29,30]. This is important because it may suggest different therapeutic strategies, changing classical approaches. Among cardiac arrhythmias, one can cite premature beats, atrial fibrillation, bradycardia, tachycardia and ventricular arrhythmias, as fibrillations and tachycardia.

The clinical arrhythmias that have the greatest potential for therapeutic applications of chaos theory are the aperiodic tachyarrhythmias, including atrial and ventricular fibrillation. Since chaotic responses may be controlled by an efficient way using control procedures [5,6,18,19,26], this may inspire some interesting approaches in order to stabilize unstable orbits associated with the normal heart rhythm. Garfinkel et al. [9,10] discuss the application of chaos control techniques in

* Corresponding author.
E-mail addresses: sandrarregina@hotmail.com (S.R.F.S.M. Gois), savi@mecanica.ufrj.br (M.A. Savi).

0960-0779/$ - see front matter © 2008 Elsevier Ltd. All rights reserved.
doi:10.1016/j.chaos.2008.09.040

order to avoid heart arrhythmic responses. This approach may be incorporated into pacemakers, avoiding ventricular fibrillation, for example.

There are different forms to evaluate the heart functioning by the measurement of some signal. An electrocardiogram (ECG) records the electrical activity of the heart being used to measure the rate and regularity of heartbeats as well as the size and position of the chambers. The electrical impulses related to the heart functioning are recorded in the form of waves, which represents the electrical current in different areas of heart [17].

Mathematical modeling of cardiac rhythms is the objective of many research efforts. Since the qualitative features of the heart actuation potential is close related to the dynamical response of the classical Van der Pol (VdP) oscillator [27], this oscillator may be considered as the starting point of this modeling. Actually, the classical article due to Van der Pol and Van der Mark [28,27] describes the heart behavior from coupled VdP oscillators. Afterwards, Hodkin and Huxley [13] describes the heartbeat behavior by considering different models. Recently, Grudzinski and Zebrowski [12] proposes a variation of the classical Van der Pol oscillator in order to capture some important aspects regarding the heart action potential. Santos et al. [23] use coupled oscillators in order to describe general aspects of heartbeat rhythms discussing different coupling terms. Campbell and Wang [3] presents a discussion dealing with some coupling characteristics of these oscillators highlighting the importance to consider time delay coupling [7].

Other modeling efforts may be found in the literature including different aspects of the heart rhythms as for example spatiotemporal characteristics. Holden and Poole [20] showed that the electrical activity of the heart can be reconstructed at different levels and time scales, by means of different types of mathematical models, including eikonal equations, partial and ordinary differential equations, and coupled lattices of maps or ordinary differential equations. Boyett et al. [2] present a model of the sinoatrial nodal and the atrial tissue in order to explain the observations about the modulation of sinoatrial activity by introduction of chemicals. More recently, Holden and Biktashev [14] and Poole et al. [21] discuss the general problem of comparing and integrating computational models of cardiac tissue at different levels of physiological detail. A general theory of synchronous concurrent algorithms is used to model spatially extended biological systems.

This paper proposes a mathematical model to describe heart rhythms by considering three coupled modified VdP oscillators. Time delay coupling is assumed in order to reproduce ECG signals and, therefore, the heart dynamics is represented by a system of differential difference equations. Numerical simulations are carried out by considering an adapted classical Runge–Kutta method. Results show that the mathematical model captures the general behavior of the heart rhythm reproducing normal and pathological responses. Pathological rhythms are simulated by considering proper variations on either the coupling terms that represents communications aspects in the heart electric system or forcing excitation that is associated with external pacemaker excitation.

2. Heart and its electrical activity

The heart walls are composed by the cardiac muscle, called myocardium, and also by striations that is similar to the skeletal muscle. Basically, the heart consists of four compartments: the right and left atria (upper part) and the right and left ventricles (lower part) (Fig. 1). The blood returns from the systemic circulation to the right atrium and from there goes to the right ventricle, where it is ejected to the lungs. Oxygenated blood returns from the lungs to the left atrium, and from there to the left ventricle. Finally, blood is pumped through the aortic valve to the aorta and to the systemic circulation.

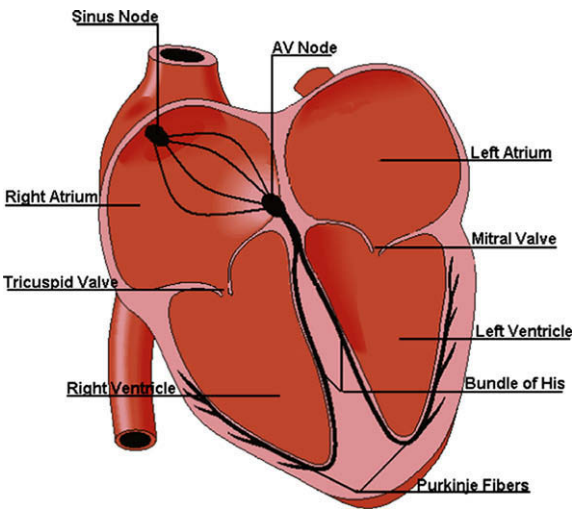

Fig. 1. Schematic picture of the heart [16].

The heart muscle cell (myocyte) has an electric activation that takes place by means of the inflow of sodium ions across the cell membrane. A plateau phase follows cardiac depolarization and, thereafter, repolarization takes place, which is a consequence of the outflow of potassium ions. The mechanical contraction of the heart is associated with the electric activation of cardiac muscle cell.

All heart rhythms are governed by activation potentials controlled by specialized cells. The sinus node (sinoatrial or SA node) is located in the right atrium at the superior vena cava (Fig. 1). The SA nodal cells are self-excitatory pacemaker cells, which generate an action potential. Activation propagates from the SA node throughout the atria, but cannot propagate directly across the boundary between atria and ventricles. The atrio-ventricular node (AV node) is located at the boundary between the atria and ventricles (Fig. 1). In a normal heart, the AV node provides the only conducting path from atria to ventricles. Therefore, under normal conditions, ventricles can be excited only by pulses that propagate through it. Propagation from the AV node to the ventricles is provided by a specialized conduction system. Proximally, this system is composed of a common bundle, called the bundle of His. More distally, it separates into two bundle branches propagating along each side of the septum, constituting the right and left bundle branches. Even more distally the bundles ramify into Purkinje fibers that diverge to the inner sides of the ventricular walls.

2.1. Activation potential

The heart electric activity is close related to cellular rhythms regulated by the Na–K pump. The concentration of sodium ions (Na+) is about 10 times higher outside the cellular membrane than inside, whereas the concentration of the potassium (K+) ions is about 30 times higher inside when compared to outside. By stimulating the membrane, the transmembrane potential rises about 20 mV and reaches the threshold, that is, when the membrane voltage changes from -70 mV to about -50 mV, the sodium and potassium ionic permeability of the membrane change. Fig. 2 presents a schematic picture of the ionic flow that generates the activation potential [14]. The sodium ion permeability increases very rapidly at first, allowing sodium ions to flow from outside to inside, increasing the inside positive potential, reaching about +20 mV. After that, there is a slowly increasing of potassium ion permeability allowing potassium ions to flow from inside to outside, causing the return of the intracellular potential to its resting value. The maximum excursion of the membrane voltage during activation is about 100 mV; the duration of the impulse is around 300 ms. While at rest, following activation, the Na–K pump restores the ion concentrations inside and outside the membrane to their original values.

Different groups of cells present different configurations of ionic channels, which lead to distinct action impulse velocities. Therefore, cells are classified as *slow* or *fast* response action potential cells that present different shapes for the action

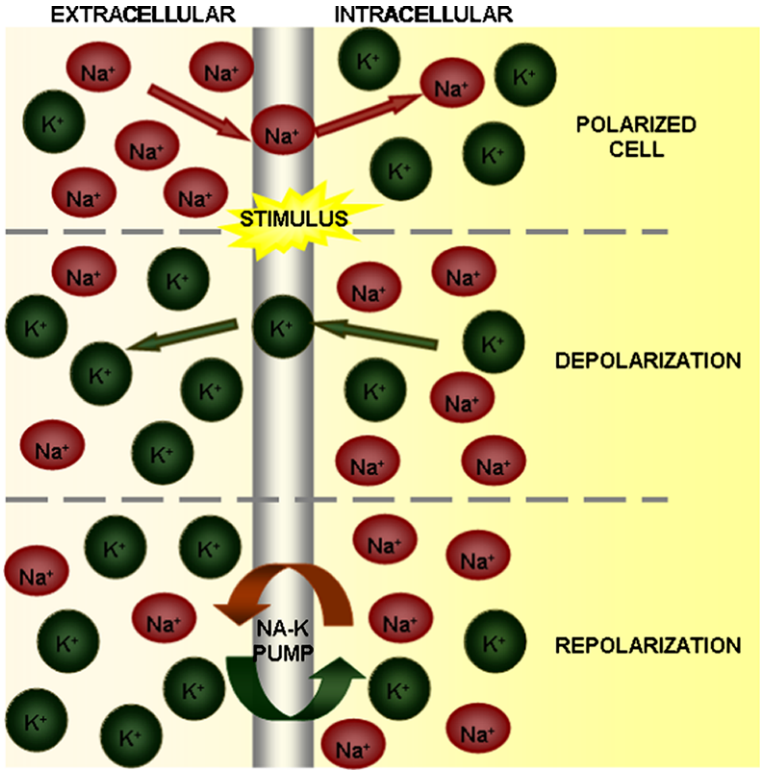

Fig. 2. The Na–K pump and the activation potential [16].

potential signal. The first group – slow response – includes the atrial and ventricular muscle, *His bundle* and *Purkinje fibers* while the second – fast response – are the SA and AV nodes [7].

The heart electric activity is related to depolarization and repolarization waves. The sodium influx is triggered by the very large and rapid rise in sodium permeability. This current is confined to a zone called the depolarization zone. The current outflow initially depolarizes the resting tissue, advancing in the direction of propagation. When a cell depolarizes, it produces an electric field which triggers the depolarization phenomenon in another cell close to it, which then depolarizes. Therefore, the depolarization may be understood as a propagating wave within cardiac tissue. The nature of the repolarization wave is different from that of the depolarization wave. Unlike depolarization, the repolarization is not a propagating phenomenon, however, by examining the location of repolarizing cells at consecutive time instances, it is possible to approximate the repolarization with a proceeding wave phenomenon.

3. Electrocardiogram (ECG)

Cardiac electric signals on an intracellular level may be recorded with a microelectrode, which is inserted inside a cardiac muscle cell. Besides, it is possible to record the electric potential generated by the heart electrical activity on the thorax surface. The ECG is a measure of the extra-cellular electric behavior of the cardiac muscle tissue. The propagation wave-front of the cardiac electrical signal through the body presents a very complicated shape. Many cardiac signal measurement systems are already proposed where leads are used to measure potential difference between points on the body surface. Actually, the measured signal is the projection of the dipole along the line defined by the leads. Therefore, depending on the leads configuration, different measurements are obtained but, in general, the signal contains the following waves:

- *P-Wave*: It is the first wave registered in the ECG, representing the atrium activation just after the sinus stimulation. It normally lasts between 60 and 90 ms in adults, has a round shape with maximal amplitude between 0.25 and 0.30 mV.
- *PR-Interval*: It is measured from the start of the P-wave to the start of the QRS-Complex and lasts 90 ms.
- *QRS-Complex*: It corresponds to the ventricular activation and is measured from the start of the first wave (no matter if it is Q- or R-wave), to the last wave (R- or S-wave). In normal adults, the complex lasts about 80 ms and presents a sharp shape because of the high frequencies of the signal. Its shape varies a lot, depending on the lead system used.
- *ST-Interval*: It lasts from the end of the QRS-complex to the start of the T-wave and corresponds to part of the ventricular repolarization process.
- *T-Wave*: It represents the ventricular activation, has a round shape with amplitude about 0.60 mV.

From the characteristics of the electric cardiac events it is possible to state the shape of each wave and their combination result in the amplitude signal of the dipole, as presented schematically in Fig. 3 [16]. The ECG is the projection of such signal according to a variable angle (the dipole orientation).

4. Mathematical modeling

The VdP equation was originally employed to describe relaxation oscillators in electronic circuits, and has been frequently used in theoretical models of the cardiac rhythm. This equation is very useful in the phenomenological modeling of natural

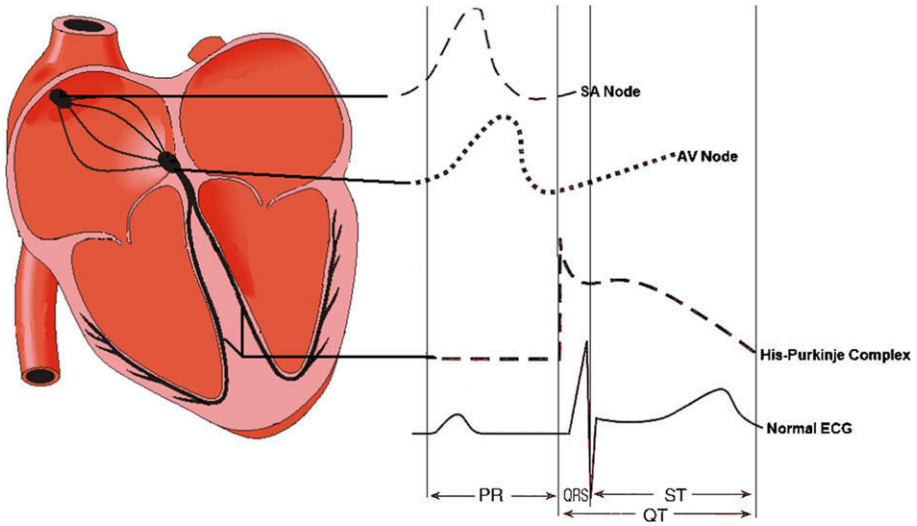

Fig. 3. Different waveforms for each of the specialized cells found in the heart [16].

systems, especially the heartbeat, since it displays many of those features supposed to occur in the biological setting as limit cycle, synchronization and chaos. The general form of this equation is presented below:

$$\ddot{x} + a(1 - bx^2)\dot{x} + cx = \Gamma(t), \tag{1}$$

where a, b and c are system parameters and $\Gamma(t)$ is an external forcing.

The qualitative features of an isolated VdP oscillator present a close similarity to the features of the heart actuation potential. Both kinds of actuation potential response (slow and fast) can be easily reproduced by the VdP oscillator. Grudzinski and Zebrowski [12] proposed a modified oscillator in order to simulate important physiological features of the action potentials. In general, the new equation has two fixed points and a dissipation term asymmetric with respect to the voltage:

$$\ddot{x} + a(x - w_1)(x - w_2)\dot{x} - \frac{x(x + d)(x + e)}{ed} = \Gamma(t), \tag{2}$$

here a, d, e, w_1 and w_2 are system parameters and $\Gamma(t)$ is an external forcing.

As already mentioned, the normal cardiac rhythm is primarily generated by the SA node, which is considered as the normal pacemaker. Besides, the AV node is another pacemaker. Each one of these presents an actuation potential that is fundamental to the heart dynamics, but not necessarily the most expressive to compose the ECG signal. Each activation (depolarization followed by repolarization) corresponds to a different region of the heart and, as a consequence, generates currents of different magnitudes. Therefore, the combination of activation waves coming from each region of the heart is responsible for the ECG form and some of these signals may be preponderant in this composition, like the waves originated in the atrium and ventricle. On the other hand, as these regions follow very close the activation of the SA and AV nodes, their signature on the ECG signal is representative of the pacemakers' signals and it is possible to associate these signals with atrium and ventricle, respectively.

Under these assumptions, it is expected that coupled oscillators, each one representing a different heart region signal, may represent the general heartbeat dynamics. Usually, two oscillators are considered representing the SA and AV nodes, however, it is observed that these two oscillators are not enough to reproduce the ECG signal. This is because the signal of the first oscillator corresponds to the activation of the SA node and atrium, and the signal of the second oscillator corresponds just to the ventricle depolarization. Under this assumption, it is possible to reproduce the *P*-curve but not the QRS-complex, because this interval mainly corresponds to the ventricle repolarization.

This observation motivate the inclusion of a third oscillator that represent the pulse propagation through the ventricles, which physiologically represents the His–Purkinje complex, composed by the His bundle and the Purkinje fibers. Fig. 4 presents the conceptual model showing either the oscillators or the coupling among them. In order to build a general model, bidirectional asymmetric couplings are assumed among all oscillators. Moreover, external excitations are incorporated to the system, considering a periodic driving term on each oscillator, $\Gamma_i(t)$. This conceptual model may be represented by a set of differential equations as follows:

$$\begin{aligned}
\dot{x}_1 &= x_2,\\
\dot{x}_2 &= -a_{\mathrm{SA}}x_2(x_1 - w_{\mathrm{SA}_1})(x_1 - w_{\mathrm{SA}_2}) - x_1(x_1 + d_{\mathrm{SA}})(x_1 + e_{\mathrm{SA}}) + \rho_{\mathrm{SA}}\sin(\omega_{\mathrm{SA}}t)\\
&\quad + k_{\mathrm{SA-AV}}(x_1 - x_3) + k_{\mathrm{SA-HP}}(x_1 - x_5)\\
\dot{x}_3 &= x_4,\\
\dot{x}_4 &= -a_{\mathrm{AV}}x_4(x_3 - w_{\mathrm{AV}_1})(x_3 - w_{\mathrm{AV}_2}) - x_3(x_3 + d_{\mathrm{AV}})(x_3 + e_{\mathrm{AV}}) + \rho_{\mathrm{AV}}\sin(\omega_{\mathrm{AV}}t)\\
&\quad + k_{\mathrm{AV-SA}}(x_3 - x_1) + k_{\mathrm{AV-HP}}(x_3 - x_5),\\
\dot{x}_5 &= x_6,\\
\dot{x}_6 &= -a_{\mathrm{HP}}x_6(x_5 - w_{\mathrm{HP}_1})(x_5 - w_{\mathrm{HP}_2}) - x_5(x_5 + d_{\mathrm{HP}})(x_5 + e_{\mathrm{HP}}) + \rho_{\mathrm{HP}}\sin(\omega_{\mathrm{HP}}t)\\
&\quad + k_{\mathrm{HP-SA}}(x_5 - x_1) + k_{\mathrm{HP-AV}}(x_5 - x_3).
\end{aligned} \tag{3}$$

These governing equations may be rewritten in a compact form as follows:

$$\ddot{y} = f(y, \dot{y}) + \Gamma(t) + Ky, \tag{4}$$

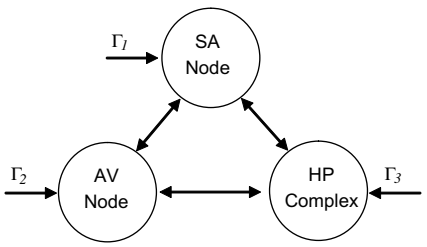

Fig. 4. Conceptual model with three coupled oscillators.

where

$$
\begin{aligned}
&y = [\,x_1 \quad x_3 \quad x_5\,]^{\mathrm{T}} \qquad \dot{y} = [\,x_2 \quad x_4 \quad x_6\,]^{\mathrm{T}} \\
&\Gamma = [\,\rho_{\mathrm{SA}}\sin(\omega_{\mathrm{SA}}t) \quad \rho_{\mathrm{AV}}\sin(\omega_{\mathrm{AV}}t) \quad \rho_{\mathrm{HP}}\sin(\omega_{\mathrm{HP}}t)]^{\mathrm{T}} \\
&K = \begin{bmatrix} k_{\mathrm{SA-AV}} + k_{\mathrm{SA-HP}} & -k_{\mathrm{SA-AV}} & -k_{\mathrm{SA-HP}} \\ -k_{\mathrm{AV-SA}} & k_{\mathrm{AV-SA}} + k_{\mathrm{AV-HP}} & -k_{\mathrm{AV-HP}} \\ -k_{\mathrm{HP-SA}} & -k_{\mathrm{HP-AV}} & k_{\mathrm{HP-SA}} + k_{\mathrm{HP-AV}} \end{bmatrix}.
\end{aligned} \tag{5}
$$

Notice that the governing equations have a general form $f(y,\dot{y})$ (related to the modified VdP oscillator), $\Gamma(t)$ is the forcing term and K represents the coupling matrix.

Time delays in signal transmission are unavoidable and, since even small delays may alter the system dynamics, it is necessary to understand how conduction delays change the behavior of coupled oscillators. The inclusion of time delays in differential equations can cause drastic changes and can make chaos emerges in a system that would otherwise be described by a regular behavior [3]. On this basis, the proposed mathematical model is changed in order to consider delay aspects in coupling terms. Therefore, governing equations are changed as follows:

$$
\begin{aligned}
\dot{x}_1 &= x_2, \\
\dot{x}_2 &= -a_{\mathrm{SA}}x_2(x_1 - w_{\mathrm{SA}_1})(x_1 - w_{\mathrm{SA}_2}) - x_1(x_1 + d_{\mathrm{SA}})(x_1 + e_{\mathrm{SA}}) + \rho_{\mathrm{SA}}\sin(\omega_{\mathrm{SA}}t) \\
&\quad + k_{\mathrm{SA-AV}}(x_1 - x_3^{\tau_{\mathrm{SA-AV}}}) + k_{\mathrm{SA-HP}}(x_1 - x_5^{\tau_{\mathrm{SA-HP}}}), \\
\dot{x}_3 &= x_4, \\
\dot{x}_4 &= -a_{\mathrm{AV}}x_4(x_3 - w_{\mathrm{AV}_1})(x_3 - w_{\mathrm{AV}_2}) - x_3(x_3 + d_{\mathrm{AV}})(x_3 + e_{\mathrm{AV}}) + \rho_{\mathrm{AV}}\sin(\omega_{\mathrm{AV}}t) \\
&\quad + k_{\mathrm{AV-SA}}(x_3 - x_1^{\tau_{\mathrm{AV-SA}}}) + k_{\mathrm{AV-HP}}(x_3 - x_5^{\tau_{\mathrm{AV-HP}}}), \\
\dot{x}_5 &= x_6, \\
\dot{x}_6 &= -a_{\mathrm{HP}}x_6(x_5 - w_{\mathrm{HP}_1})(x_5 - w_{\mathrm{HP}_2}) - x_5(x_5 + d_{\mathrm{HP}})(x_5 + e_{\mathrm{HP}}) + \rho_{\mathrm{HP}}\sin(\omega_{\mathrm{HP}}t) \\
&\quad + k_{\mathrm{HP-SA}}(x_5 - x_1^{\tau_{\mathrm{HP-SA}}}) + k_{\mathrm{HP-AV}}(x_5 - x_3^{\tau_{\mathrm{HP-AV}}}),
\end{aligned} \tag{6}
$$

where $x_i^{\tau} = x_i(t-\tau)$ and τ represents the time delay. Notice that, actually, there are different delays depending on the connection type. The general idea of these coupled oscillators is that the ECG signal is built from the composition of these signals as follows:

$$
X = \mathrm{ECG} = \alpha_0 + \alpha_1 x_1 + \alpha_3 x_3 + \alpha_5 x_5. \tag{7}
$$

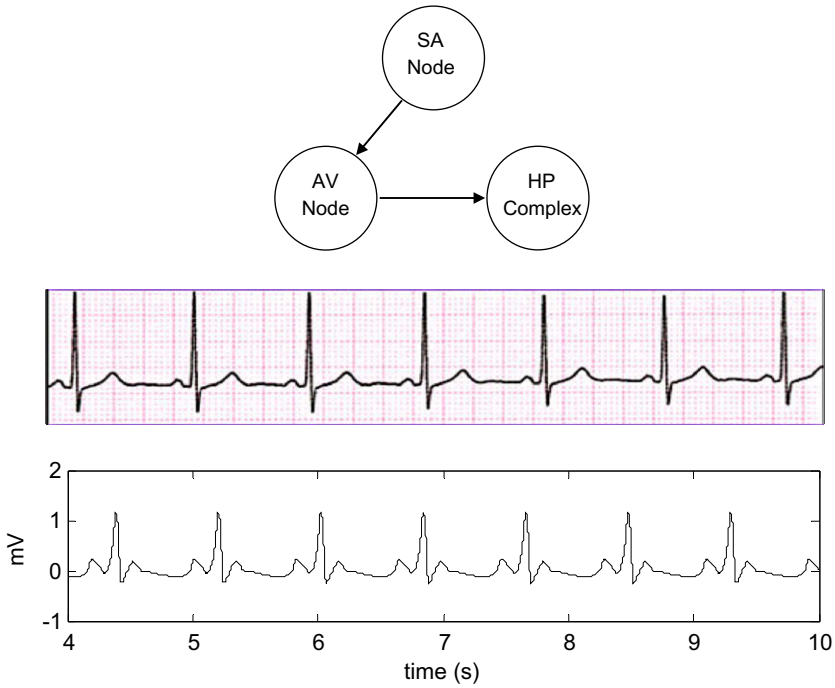

Fig. 5. Normal ECG.

Analogously, it is possible to define

$$\dot{X} = \frac{\mathrm{d(ECG)}}{\mathrm{d}t} = \alpha_1 x_2 + \alpha_3 x_4 + \alpha_5 x_6. \tag{8}$$

Numerical procedure employed to deal with these difference differential equations is an adapted classical fourth-order Runge–Kutta method. Basically, by considering the system $\ddot{y} = f(y, \dot{y}) + \Gamma(t) + K[y - y^{\tau}]$, it is assumed a function equivalent to the delayed system and, for time instants $t < \tau$, the function y_0 provides values corresponding to time delays prior to the initial instant of observation [1]:

$$y_0(t) = y(t - \tau). \tag{9}$$

The determination of $y_0(t)$ may be done using Taylor's series, approximating the exact solution as follows [4]:

$$y(t - \tau) \cong y(t) - \tau\dot{y}(t) + \frac{\tau^2}{2}\ddot{y}(t). \tag{10}$$

Under this assumption, it is possible to obtain approximated values for $y(t - \tau)$ at least in the time interval $t < \tau$. After this, it is possible to use the integrated values in order to construct the time delayed function.

5. Numerical simulations

This section considers numerical simulations performed with the proposed heart model. Parameter values suggested by [12,23] are used as reference values of the SA node oscillator for the normal ECG. The other parameters are adjusted in order to qualitatively match real ECG signals captured from the second derivation, which are available in [15,31]. It is beyond the scope of this contribution an automatic determination of the system parameters. Here, the parameter choices are done in an artisanal way, with the objective to understand the heart rhythms by a dynamical point of view and therefore, the interest is essentially in the qualitative system response. Under this consideration, the following parameters are adopted to represent

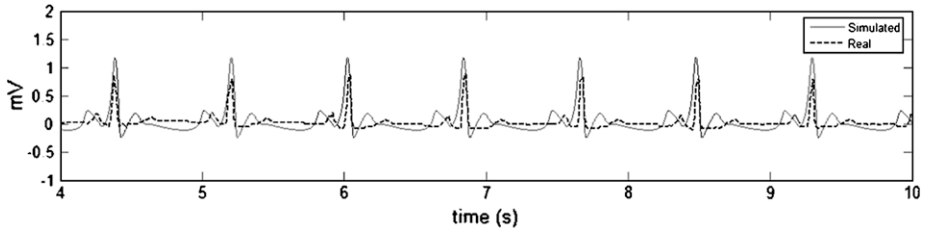

Fig. 6. Real and simulated normal ECG comparison.

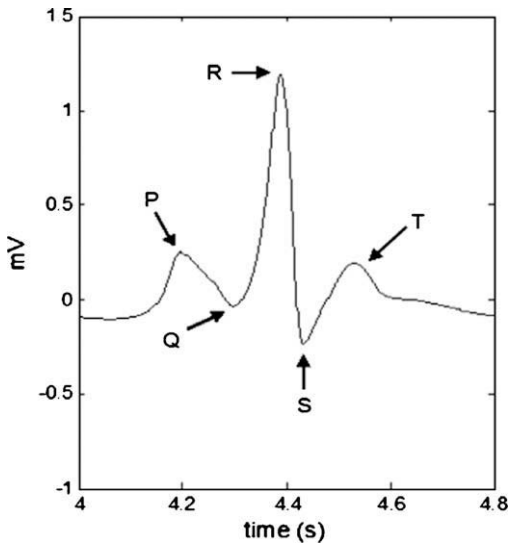

Fig. 7. Simulated normal ECG detailed view.

the normal heart functioning: $a_{SA} = 3$, $w_{SA_1} = 0.2$, $w_{SA_2} = -1.9$, $d_{SA} = 3$, $e_{SA} = 4.9$; $a_{AV} = 3$, $w_{AV_1} = 0.1$, $w_{AV_2} = -0.1$, $d_{AV} = 3$, $e_{AV} = 3$; $a_{HP} = 5$, $w_{HP_1} = 1$, $w_{HP_2} = -1$, $d_{HP} = 3$, $e_{HP} = 7$ $\alpha_0 = 1$, $\alpha_1 = 0.1$, $\alpha_3 = 0.05$, $\alpha_5 = 0.4$.

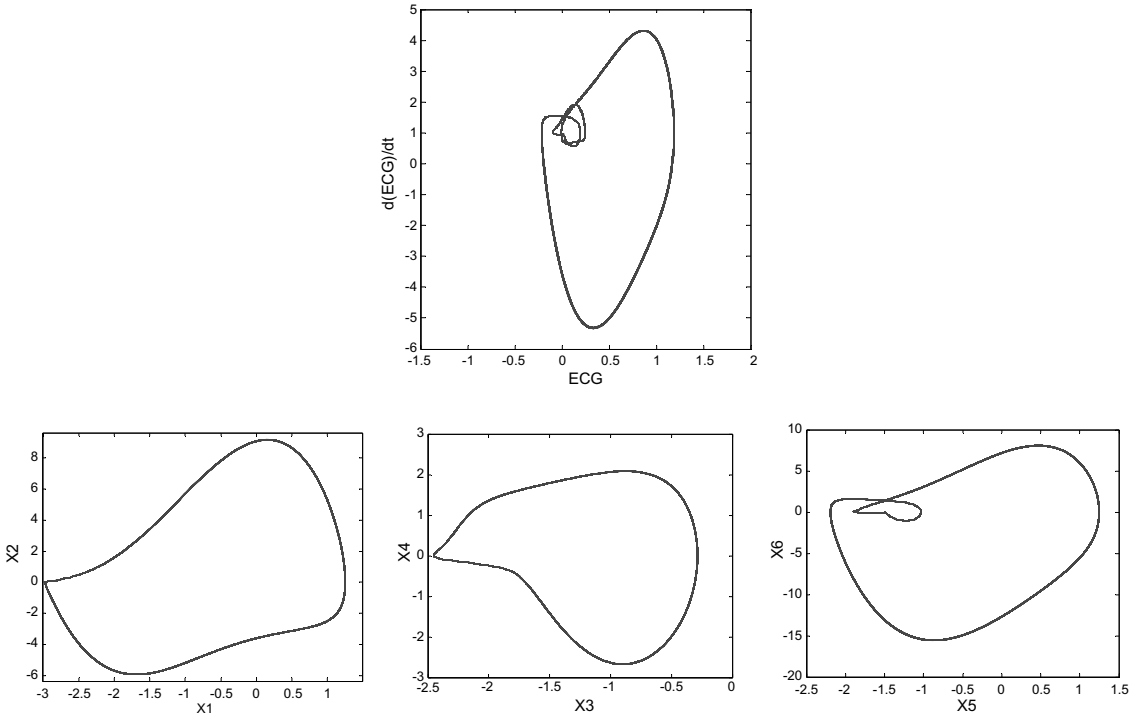

Fig. 8. Phase space plots related to the normal ECG.

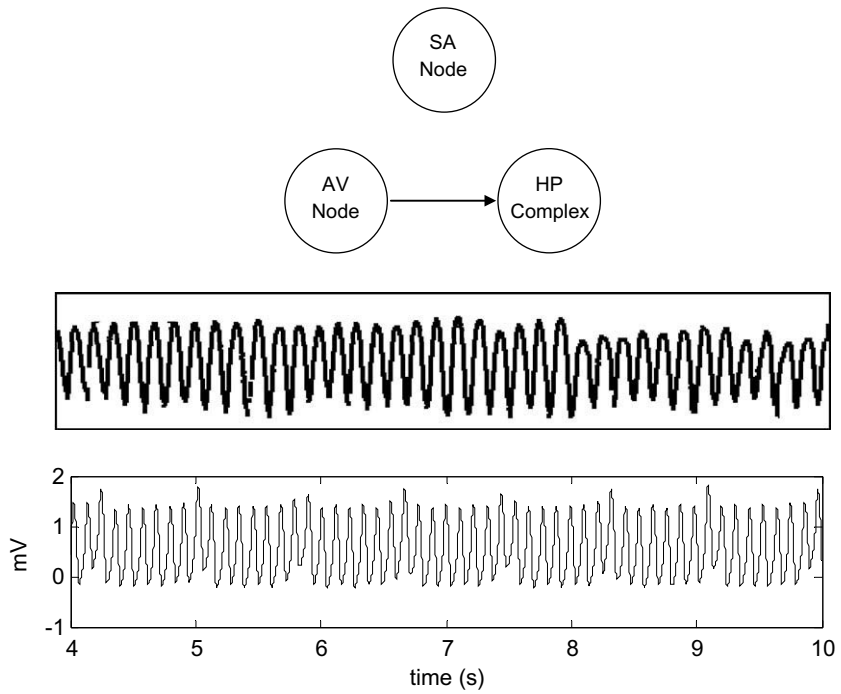

Fig. 9. ECG without SA–AV coupling (ventricular flutter).

Concerning coupling aspects, it is assumed that the normal heart has a unidirectional coupling from SA to AV nodes and also from AV to HP. Therefore, $k_{SA-AV} = 5$ and $k_{AV-HP} = 20$ are non-vanishing terms and all other couplings vanishes. Moreover,

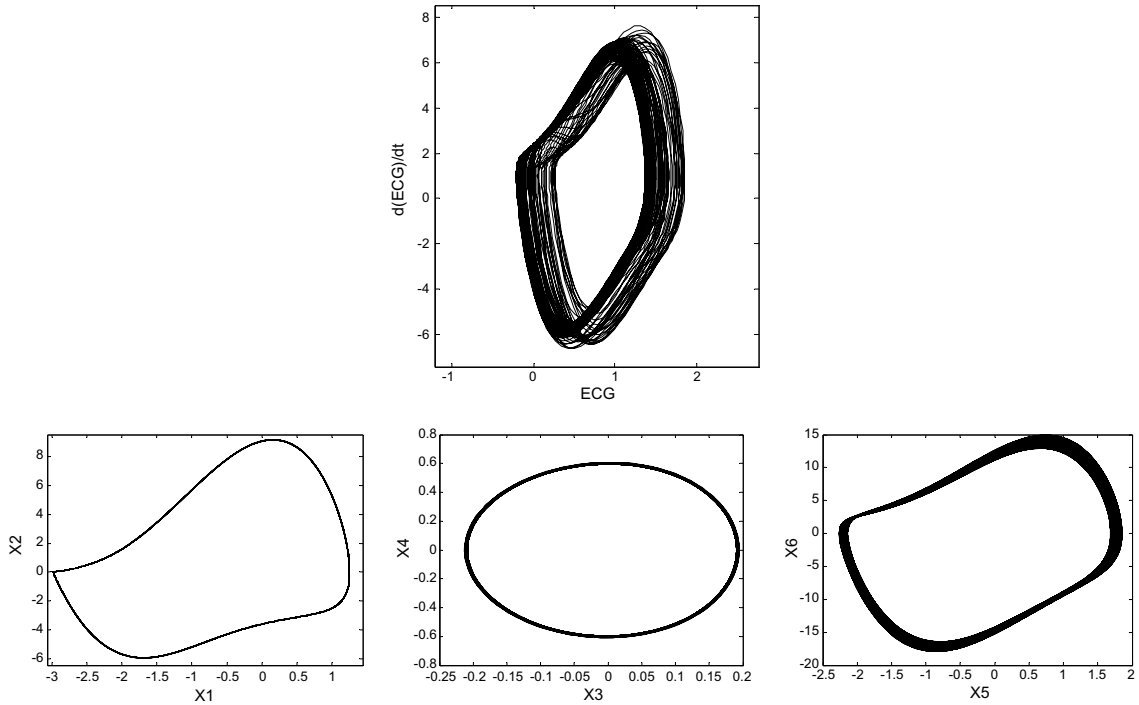

Fig. 10. Phase space plots related to the ventricular flutter.

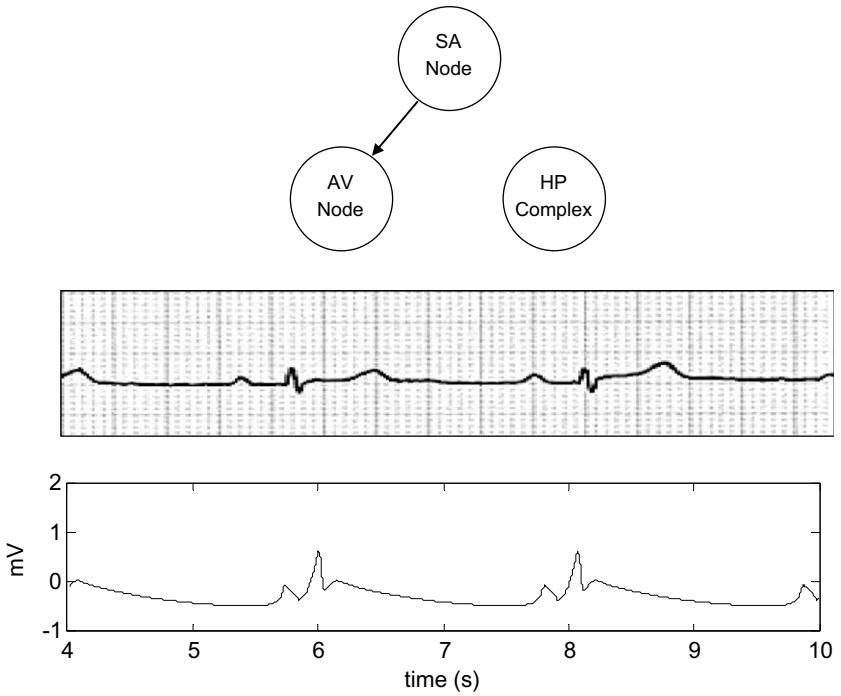

Fig. 11. ECG without AV–HP coupling (sinus bradycardia).

it is necessary to establish proper coupling time delay parameters. If there is no coupling, the time delay does not matter. In this regard, the following parameters are assumed: $\tau_{SA-AV} = 0.8$ and $\tau_{AS-HP} = 0.1$, vanishing all others.

Under this condition, the ECG simulation is carried out and the result is presented in Fig. 5 showing schematic heart functioning and the time history of the resultant signal. Besides, it is presented a real ECG captured at the second derivation [15].

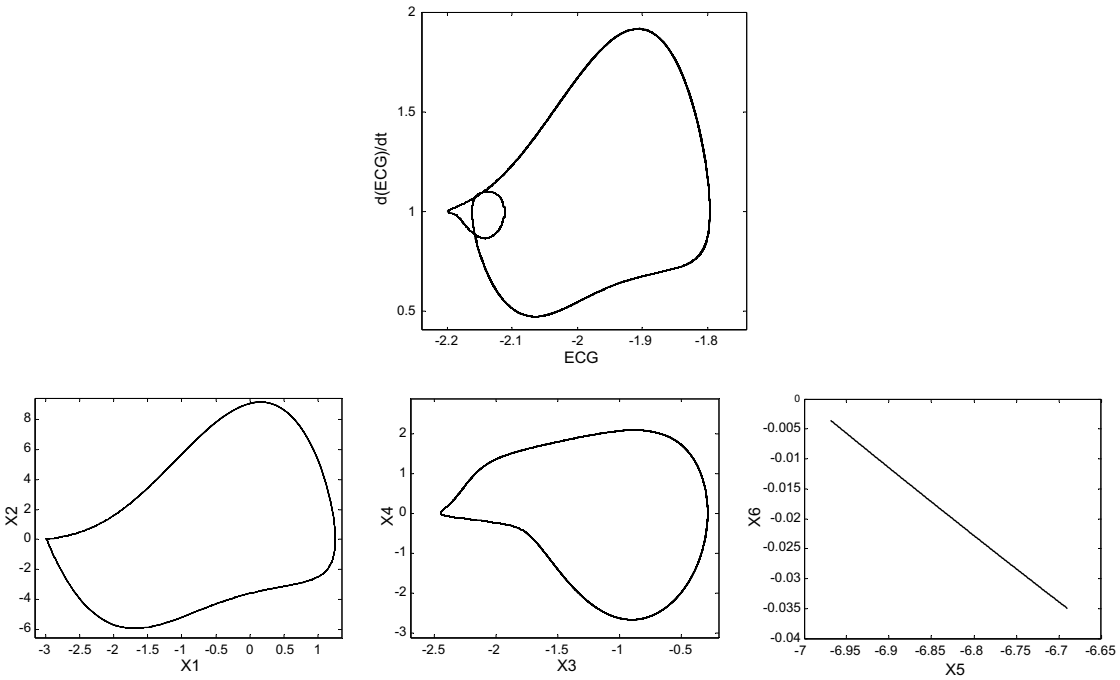

Fig. 12. Phase space plots related to the sinus bradycardia.

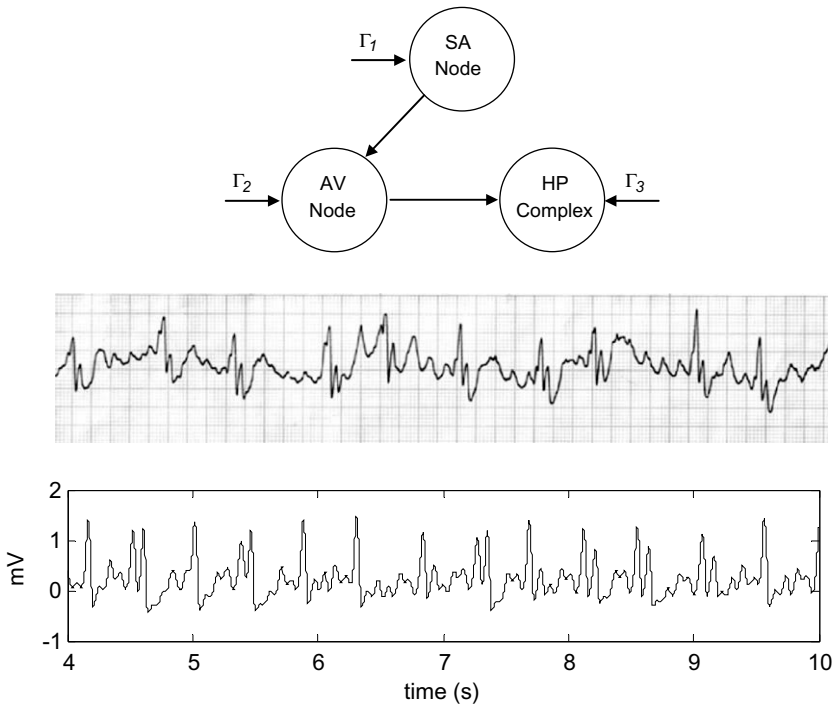

Fig. 13. ECG with external pacemaker excitation (ventricular fibrillation).

By comparing numerical simulation with the real ECG, it is possible to observe that they are in qualitative agreement. Fig. 6 presents a comparison between the real and the simulated ECG, showing that the model is able to capture the general behavior of the real ECG, and the numerical simulation matches the real measurements. These conclusions are clearer observing an enlargement of the simulated normal ECG presented in Fig. 7, showing that it captures its general characteristics, presenting the most important waves: P, QRS, T.

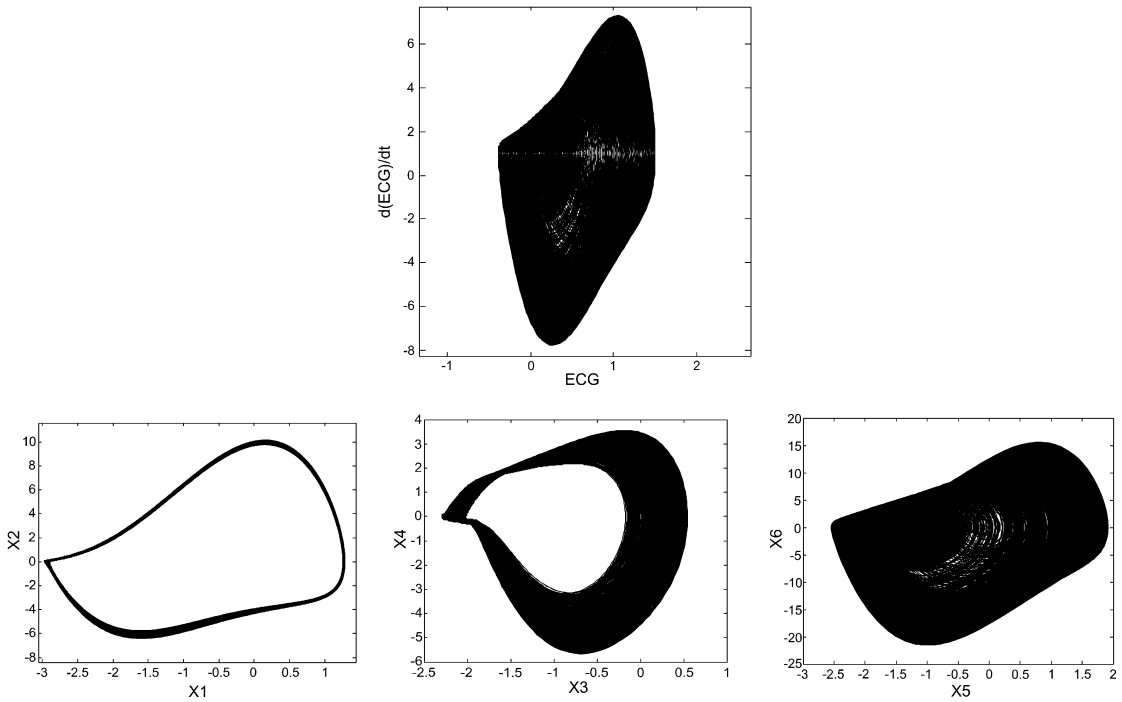

Fig. 14. Phase space plots related to the ventricular fibrillation.

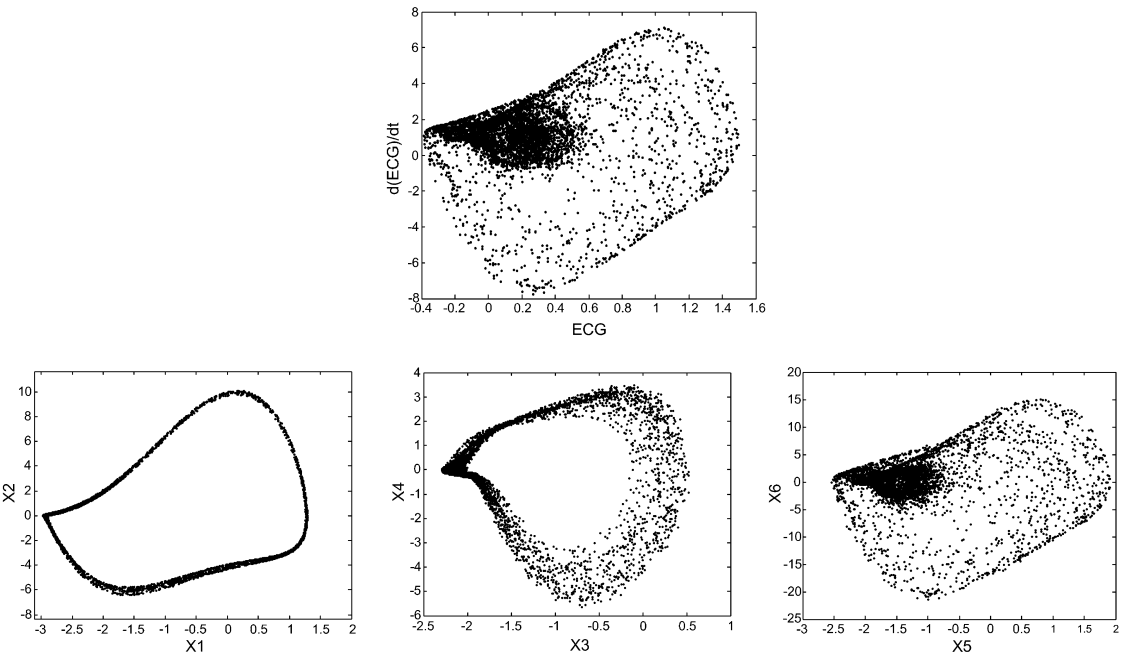

Fig. 15. Poincaré maps related to ventricular fibrillation.

The system dynamics may be better understood observing phase space plots. The phase space plot of the normal ECG is essentially periodic (Fig. 8). Fig. 8 also shows the phase space two-dimensional projections of the general six-dimensional space, representing the dynamics of each oscillator (SA, AV and HP). The periodic characteristic of the behavior is again noticeable.

The forthcoming analysis treats different coupling terms in order to simulate some heart pathologies identified from ECG. At first, it is considered the case where there is no communication between the SA and AV nodes, what is simulated by eliminating the coupling between the first and second oscillators ($k_{AV-SA} = 0$), while the value of all other parameters are the same as in the normal ECG. Under this condition, the system is driven by the AV node, presenting a higher frequency rhythm when compared with the normal ECG. This pathology is called *ventricular flutter* presenting a typical ECG form. Fig. 9 presents the numerical simulation together with a real ECG [15]. Fig. 10 presents the phase space plots and some of their two-dimensional projections associated with this response, confirming its irregular characteristic. This irregularity suggests a chaotic-like response that, however, should be assured by some system invariant as the Lyapunov exponent.

The AV–HP coupling is now in focus and the only non-vanishing coupling term is $k_{SA-AV} = 5$, which means that k_{HP-AV} vanishes. Under this condition, the ventricles influence is different and the heart rhythm is represented by the ECG showed in Fig. 11, usually called *sinus bradycardia* [15]. This kind of pathology has a regular behavior as can be observed in the phase space plots and some of their two-dimensional projections presented in Fig. 12.

At this point, the normal ECG is considered again, however, external pacemakers are exciting the heartbeat. Therefore, it is considered the same parameters related to the normal ECG (Figs. 6–8) together with the following forcing parameters: $e_{SA} = 6$, $\rho_{SA} = 1$, $\rho_{AV} = 1$, $\rho_{HP} = 20$, $\omega_{SA} = \omega_{AV} = \omega_{HP} = 2\pi/(60/70)$. Under this condition, a behavior called *ventricular fibrillation* is induced. This pathological response is caused by different ventricle stimulation being characterized by irregular ECG with fast QRS response. Fig. 13 shows the numerical simulation related to this condition together with a typical real ECG [15].

Phase space plots and some of their two-dimensional projections of this ventricular fibrillation response are presented in Fig. 14. The irregular characteristic of this kind of behavior is noticeable since the response is not related to a closed curve. By analyzing the Poincaré maps, chaotic-like structure is suggested (Fig. 15). Since the response seems to be chaotic, this conclusion should be confirmed by analyzing some system invariant as the Lyapunov exponent.

6. Conclusions

A mathematical modeling of heart rhythm dynamics is developed considering three modified VdP oscillators connected by time delay coupling. Each oscillator represents one of the most important heart natural pacemakers: sinoatrial node (SA), atrio-ventricular node (AV) and His–Purkinje complex (HP). The resulting differential difference equations are integrated by considering an estimation of the time delayed system function with the aid of the Taylor's series. Numerical simulations are carried out showing that the proposed model is capable to capture the general heartbeat dynamics, representing the normal ECG form with P, QRS and T waves. Afterwards, some pathological rhythms are of concern by establishing different coupling situations. Basically, it is assumed some communication interruption in the heart electric system. Under this condition, it is possible to simulate cardiopathologies as ventricular flutter and sinus bradycardia. Moreover, external pacemaker excitation is of concern representing other pathological behaviors as the ventricular fibrillation. These results show that the three oscillator model captures the general behavior of heart rhythms represented by ECG signals and may encourage the identification of different pathological rhythms. Besides, it is shown that the dynamical approach may be useful to identify system characteristics and phase space plots and Poincaré maps may highlight some kinds of behavior more than the ECG form.

Acknowledgements

The authors acknowledge the support of the Brazilian Research Councils CNPq and FAPERJ.

References

[1] Boucekkine R, Licandro O, Paul C. Differential-difference equations in economics: on the numerical solution of vintage capital growth models. J Econ Dyn Control 1997;21:347–62.
[2] Boyett MR, Holden AV, Kodama I, Suzuki R, Zhang H. Atrial modulation of sinoatrial pacemaker rate. Chaos, Solitons & Fractals 1995;5:425–38.
[3] Campbell SR, Wang D. Relaxation oscillators with time delay coupling. Physica D 1998;111:151–78.
[4] Cunningham WJ. A nonlinear differential-difference equation of growth. Proc Natl Acad Sci USA 1954;40(8):708–13.
[5] de Paula AS, Savi MA. A multiparameter chaos control method based on OGY approach. Chaos, Solitons & Fractals 2009;40(3):1376–90.
[6] de Paula AS, Savi MA. Controlling Chaos in a nonlinear pendulum using an extended time-delayed feedback control method. Chaos, Solitons & Fractals, doi:10.1016/j.chaos.2009.04.039.
[7] Dubin D. Interpretação rápida do ECG, Editora de Publições Biomédicas – EPUB, Rio de Janeiro, 1996.
[8] Ferriere R, Fox GA. Chaos and evolution. Trends Ecol Evol 1995;10(12):480–5.
[9] Garfinkel A, Spano ML, Ditto WL, Weiss JN. Controlling cardiac chaos. Science 1992;257:1230–5.
[10] Garfinkel A, Weiss JN, Ditto WL, Spano ML. Chaos control of cardiac arrhythmias. Trends Cardiovasc Med 1995;5(2):76–80.
[11] Glass L. Synchronization and rhythmic processes in physiology. Nature 2001;410(March):277–84.
[12] Grudzinski K, Zebrowski JJ. Modeling cardiac pacemakers with relaxation oscillators. Physica A 2004;336:153–62.
[13] Hodkin AL, Huxley AF. A quantitative description of membrane current and its application to conduction and excitation in nerve. J Physiol 1952;117:500–44.
[14] Holden AV, Biktashev VN. Computational biology of propagation in excitable media models of cardiac tissue. Chaos, Solitons & Fractals 2002;13:1643–58.

[15] Jenkins D, Gerred S. ECG library. Available from: <http://www.ecglibrary.com>, 2007.
[16] Malmivuo J, Plonsey R. Bioelectromagnetism – principles and applications of bioelectric and biomagnetic fields. New York: Oxford University Press; 1995.
[17] Moffa PJ, Sanches PCR. Eletrocardiograma normal e patológico. Editora Roca 2001.
[18] Pereira-Pinto FHI, Ferreira AM, Savi MA. Chaos control in a nonlinear pendulum using a semi-continuous method. Chaos, Solitons & Fractals 2004;22(3):653–68.
[19] Pereira-Pinto FHI, Ferreira AM, Savi MA. State space reconstruction using extended state observers to control chaos in a nonlinear pendulum. Int J Bifurc Chaos 2005;15(12):4051–63.
[20] Poole MJ, Holden AV, Tucker JV. Reconstructing the heart. Chaos, Solitons & Fractals 1995;5:691–704.
[21] Poole MJ, Holden AV, Tucker JV. Hierarchical reconstructions of cardiac tissue. Chaos, Solitons & Fractals 2002;13:1581–612.
[22] Radhakrishna RKA, Dutt DN, Yeragani VK. Nonlinear measures of heart rate time series: influence of posture and controlled breathing. Auton Neurosci Basic Clin 2000;83:148–58.
[23] Santos AM, Lopes SR, Viana RL. Rhythm synchronization and chaotic modulation of coupled Van der Pol oscillators in a model for the heartbeat. Physica A 2004;338:335–55.
[24] Savi MA. Chaos and order in biomedical rhythms. J Braz Soc Mech Sci Eng 2005;XXVII(2):157–69.
[25] Savi MA. Nonlinear dynamics and chaos, Editora E-papers, 2006 (in Portuguese).
[26] Savi MA, Pereira-Pinto FHI, Ferreira AM. Chaos control in mechanical systems. Shock Vibr 2006;13(4/5):301–14.
[27] Van Der Pol B. On relaxation oscillations. Philos Mag 1926;2:978.
[28] Van Der Pol B, Van Der Mark J. The heartbeat considered as a relaxation oscillator and an electrical model of the heart. Philos Mag 1928;6(Suppl.):763.
[29] Witkowski FX, Kavanagh KM, Penkoske PA, Plonsey R, Spano ML, Ditto WL, et al. Evidence for determinism in ventricular fibrillation. Phys Rev Lett 1995;75(6):1230–3.
[30] Witkowski FX, Leon LJ, Penkoske PA, Giles WR, Spano ML, Ditto WL, et al. Spatiotemporal evolution of ventricular fibrillation. Nature 1998;392(March):78–82.
[31] Yanowitz FG. ECG learning center in cyberspace. Available from: <http://library.med.utah.edu/kw/ecg/image_index>, 2007.